Chapter 2
Electrochemistry of the Chalcogens

2.1 General References

Because of their multiple oxidation states, the chalcogens, particularly sulfur, can engage in numerous redox couples participating in acid–base, oxidation–reduction, precipitation, and complexation equilibria.

In the anion electrochemical series, sulfur, being the less noble element compared to its heavier congeners, occupies an intermediate position between iodine and selenium [(+)F, Cl, Br, I, S, Se, Te(–)]. Selenium, regarded as a metalloid, is a relatively noble element. Tellurium is rather an amphoteric element: it can enter into solution in the form of both cations and anions. Regarded as a metal, i.e., with respect to its cations, tellurium occupies a position between copper and mercury. Regarded as a metalloid, i.e., with respect to its anions, it is located on the extreme right of the above series.

A comprehensive survey of the classical electrochemical facts for sulfur, selenium, and tellurium, as documented until about 1970, can be found in the reviews of Zhdanov [1], wherefrom we cite the lists of standard and formal potentials for aqueous solutions, in Tables 2.1, 2.2, and 2.3, respectively. Many of these potentials have been calculated thermodynamically since the experimental determinations are few. The listed data are largely drawn from the monograph by Pourbaix (below), and the interested reader should validate the measurement conditions for the indicated potentials or the scatter in their values (not given here in detail). In these tables, the redox systems are assorted by decreasing formal valency of chalcogen in the oxidized state, while at a given valency of the oxidized state they appear in the order of decreasing valency of chalcogen in the reduced state. Latimer [2] has compiled useful aqueous redox transition potential diagrams (reproduced also in Zhdanov's monographs) that are convenient as a quick guide in practical problems and for perceiving the oxidation–reduction properties of some chalcogen hydride and oxychalcogenide species. Standard potentials of chalcogens in non-aqueous media are generally not known, at least in a systematic manner.

A standard approach for the theoretical presentation of electrochemical equilibria is the use of Pourbaix, or potential–pH predominance area diagrams, which incorporate chemical and electrochemical thermodynamics simultaneously in a straightforward manner. These diagrams comprise an extremely useful, yet fundamental,

M. Bouroushian, *Electrochemistry of Metal Chalcogenides*, Monographs in Electrochemistry, DOI 10.1007/978-3-642-03967-6_2,

starting point for the study of electrochemical systems. Certainly, the ability to predict, understand, and ultimately control electrochemical reactions requires also knowledge of process kinetics.

Reproduced below are the potential–pH diagrams for the chalcogen–water systems as originally derived and illustrated by Pourbaix [3], along with some accompanying data. These will serve as a guide to all subsequent discussion on aqueous systems used for electrochemical preparations of metal chalcogenides. The reader may take notice of the chalcogen-containing substances that are considered to be present in the electrolytes and their stability domains. The diagrams represent, almost exclusively, the important "valencies" of the chalcogens, namely –2, +4, and +6 (and not effective oxidation states corresponding, e.g., to polysulfides and the like). Still, all known substances for each chalcogen, either stable in water or not, are registered here, in order to serve as a useful basis for the formulae and nomenclature used in the rest of the book. Note that the parts of the Pourbaix diagrams outside the zero activity lines (log $C = 0$) regard ideal solutions containing 1 M of dissolved chalcogen in the forms considered, and the parts inside these lines regard solutions saturated with solid chalcogen (plus TeO_2 in the case of tellurium). The diagrams are valid only in the absence of substances with which the respective chalcogen can form soluble complexes or insoluble salts.

It is considered useful to include here the potential–pH diagram for some redox systems related to oxygen (Fig. 2.1) [4]. Lines $11'$ and $33'$ correspond to the (a) and (b) dashed lines bounding the stability region of water, as depicted in all the subsequent Pourbaix diagrams.

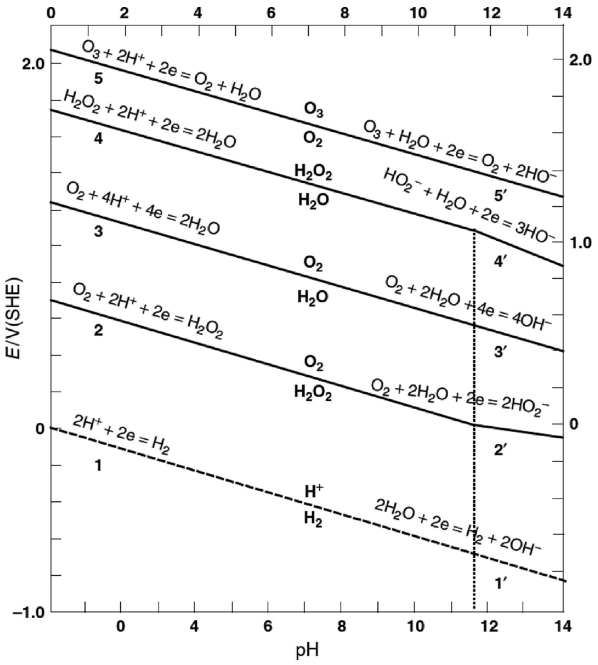

Fig. 2.1 Potential–pH diagram for oxygen reactions. (L' Her [4] Copyright Wiley-VCH Verlag GmbH & Co. KGaA. Reproduced with permission)

2.1.1 Tables of Aqueous Standard and Formal Potentials

Table 2.1 Sulfur reactions

Half-reaction	Standard or formal potential (V vs. SHE at 25 °C)
$S_2O_8^{2-} + 2e^- \rightarrow 2SO_4^{2-}$	+2.01
$S_2O_8^{2-} + 2H^+ + 2e^- \rightarrow 2\,HSO_4^-$	+2.123
$2SO_4^{2-} + 4H^+ + 2e^- \rightarrow S_2O_6^{2-} + 2H_2O$	−0.22
$SO_4^{2-} + 4H^+ + 2e^- \rightarrow H_2SO_3 + H_2O$	+0.17
$SO_4^{2-} + 4H^+ + 2e^- \rightarrow SO_2 + 2H_2O$	+0.138
$SO_4^{2-} + H_2O + 2e^- \rightarrow SO_3^{2-} + 2OH^-$	−0.93
$HSO_4^- + 7H^+ + 6e^- \rightarrow S(s) + 4H_2O$	+0.339
$SO_4^{2-} + 8H^+ + 6e^- \rightarrow S(s) + 4H_2O$	+0.357
$HSO_4^- + 9H^+ + 8e^- \rightarrow H_2S(aq) + 4H_2O$	+0.289
$SO_4^{2-} + 10H^+ + 8e^- \rightarrow H_2S(aq) + 4H_2O$	+0.303
$SO_4^{2-} + 9H^+ + 8e^- \rightarrow HS^- + 4H_2O$	+0.252
$SO_4^{2-} + 8H^+ + 8e^- \rightarrow S^{2-} + 4H_2O$	+0.149
$SO_4^{2-} + 10H^+ + 8e^- \rightarrow H_2S(g) + 4H_2O$	+0.311
$S_2O_6^{2-} + 4H^+ + 2e^- \rightarrow 2H_2SO_3$	+0.57
$S_2O_6^{2-} + 2H^+ + 2e^- \rightarrow 2HSO_3^-$	+0.455
$S_2O_6^{2-} + 2e^- \rightarrow 2SO_3^{2-}$	+0.026
$3H_2SO_3 + 2e^- \rightarrow S_3O_6^{2-} + 3H_2O$	+0.30
$2H_2SO_3 + H^+ + 2e^- \rightarrow HS_2O_4^- + 2H_2O$	−0.08, −0.056
$2SO_3^{2-} + 2H_2O + 2e^- \rightarrow S_2O_4^{2-} + 4OH^-$	−1.12
$2SO_3^{2-} + 4H^+ + 2e^- \rightarrow S_2O_4^{2-} + 2H_2O$	+0.416
$2HSO_3^- + 3H^+ + 2e^- \rightarrow HS_2O_4^- + 2H_2O$	+0.060
$2HSO_3^- + 2H^+ + 2e^- \rightarrow S_2O_4^{2-} + 2H_2O$	−0.013, −0.009
$4H_2SO_3 + 4H^+ + 6e^- \rightarrow S_4O_6^{2-} + 6H_2O$	+0.51
$4HSO_3^- + 8H^+ + 6e^- \rightarrow S_4O_6^{2-} + 6H_2O$	+0.581
$4SO_2(g) + 4H^+ + 6e^- \rightarrow S_4O_6^{-2} + 2H_2O$	+0.510
$2H_2SO_3 + 2H^+ + 4e^- \rightarrow S_2O_3^{2-} + 3H_2O$	+0.40
$2SO_3^{2-} + 3H_2O + 4e^- \rightarrow S_2O_3^{2-} + 6OH^-$	−0.58
$2SO_3^{2-} + 6H^+ + 4e^- \rightarrow S_2O_3^{2-} + 3H_2O$	+0.705
$H_2SO_3 + 2H^+ + 2e^- \rightarrow H_2SO_2 + H_2O$	< +0.4
$2HSO_3^- + 4H^+ + 4e^- \rightarrow S_2O_3^{2-} + 3H_2O$	+0.491
$5H_2SO_3 + 8H^+ + 10e^- \rightarrow S_5O_6^{2-} + 9H_2O$	+0.41
$H_2SO_3 + 4H^+ + 4e^- \rightarrow S(s) + 3H_2O$	+0.45
$SO_3^{2-} + 3H_2O + 4e^- \rightarrow S(s) + 6OH^-$	−0.66
$SO_2(g) + 4H^+ + 4e^- \rightarrow S(s) + 2H_2O$	+0.451, +0.470
$SO_3^{2-} + 6H^+ + 6e^- \rightarrow S^{2-} + 3H_2O$	+0.231
$S_4O_6^{2-} + 2e^- \rightarrow 2S_2O_3^{2-}$	+0.08, +0.219, −0.10
$S_4O_6^{2-} + 12H^+ + 10e^- \rightarrow 4S(s) + 6H_2O$	+0.416

Table 2.1 (continued)

Half-reaction	Standard or formal potential (V vs. SHE at 25 °C)
$H_2SO_2 + 2H^+ + 2e^- \rightarrow S(s) + 2H_2O$	>+0.5
$S_2O_3^{2-} + 6H^+ + 4e^- \rightarrow 2S(s) + 3H_2O$	+0.465
$S_5O_6^{2-} + 12H^+ + 10e^- \rightarrow 5S(s) + 6H_2O$	+0.484
$SO(g) + 2H^+ + 2e^- \rightarrow S(s) + H_2O$	+1.507
$5S_2O_3^{2-} + 30H^+ + 24e^- \rightarrow 2S_5^{2-} + 15H_2O$	+0.331
$S_2O_3^{2-} + 8H^+ + 8e^- \rightarrow 2HS^- + 3H_2O$	+0.200
$S_2O_3^{2-} + 6H^+ + 8e^- \rightarrow 2S^{2-} + 3H_2O$	−0.006
$S_2Cl_2 + 2e^- \rightarrow 2S(s) + 2Cl^-$	+1.23
$5S(s) + 2e^- \rightarrow S_5^{2-}$	−0.340, −0.315
$4S(s) + 2e^- \rightarrow S_4^{2-}$	−0.33
$S(s) + 2H^+ + 2e^- \rightarrow H_2S(aq)$	+0.141
$S(s) + 2H^+ + 2e^- \rightarrow H_2S(g)$	+0.171
$S(s) + H^+ + 2e^- \rightarrow HS^-$	−0.065
$S(s) + H_2O + 2e^- \rightarrow HS^- + OH^-$	−0.52
$S(s) + 2e^- \rightarrow S^{2-}$	A large number of measurements and calculated values are available. These vary from −0.48 to −0.58 V, but most are closer to −0.48 V
$4S_5^{2-} + 2e^- \rightarrow 5S_4^{2-}$	−0.441
$S_5^{2-} + 5H^+ + 8e^- \rightarrow 5HS^-$	+0.003
$S_5^{2-} + 10H^+ + 8e^- \rightarrow 5H_2S(g)$	+0.299
$3S_4^{2-} + 2e^- \rightarrow 4S_3^{2-}$	−0.478
$S_4^{2-} + 2e^- \rightarrow S^{2-} + S_3^{2-}$	−0.52
$S_4^{2-} + 4H^+ + 6e^- \rightarrow 4HS^-$	+0.033
$2S_3^{2-} + 2e^- \rightarrow 3S_2^{2-}$	−0.506
$S_3^{2-} + 2e^- \rightarrow S^{2-} + S_2^{2-}$	−0.49
$S_3^{2-} + 3H^+ + 4e^- \rightarrow 3HS^-$	+0.097
$S_2^{2-} + 2e^- \rightarrow 2S^{2-}$	−0.48, −0.524
$S_2^{2-} + 2H^+ + 2e^- \rightarrow 2HS^-$	+0.298

Table 2.2 Selenium reactions

Half-reaction	Standard or formal potential (V vs. SHE at 25 °C)
$HSeO_4^- + 3H^+ + 2e^- \rightarrow H_2SeO_3 + H_2O$	+1.090
$SeO_4^{2-} + 4H^+ + 2e^- \rightarrow H_2SeO_3 + H_2O$	+1.15
$SeO_4^{2-} + 3H^+ + 2e^- \rightarrow HSeO_3^- + H_2O$	+1.075
$SeO_4^{2-} + 2H^+ + 2e^- \rightarrow SeO_3^{2-} + H_2O$	+0.880
$SeO_4^{2-} + 2e^- + H_2O \rightarrow SeO_3^{2-} + 2OH^-$	+0.05

Table 2.2 (continued)

Half-reaction	Standard or formal potential (V vs. SHE at 25 °C)
$H_2SeO_3 + 4H^+ + 4e^- \rightarrow Se(s) + 3H_2O$	+0.740
$HSeO_3^- + 5H^+ + 4e^- \rightarrow Se(s) + 3H_2O$	+0.778
$SeO_3^{2-} + 6H^+ + 4e^- \rightarrow Se(s) + 3H_2O$	+0.875
$SeO_3^{2-} + 4e^- + 3H_2O \rightarrow Se(s) + 6OH^-$	−0.366
$Se^{4+} + 4e^- \rightarrow Se(s)$	+0.846
$H_2SeO_3 + 6H^+ + 6e^- \rightarrow H_2Se + 3H_2O$	+0.360
$HSeO_3^- + 7H^+ + 6e^- \rightarrow H_2Se + 3H_2O$	+0.386
$HSeO_3^- + 6H^+ + 6e^- \rightarrow HSe^- + 3H_2O$	+0.349
$SeO_3^{2-} + 7H^+ + 6e^- \rightarrow HSe^- + 3H_2O$	+0.414
$SeO_3^{2-} + 6H^+ + 6e^- \rightarrow Se^{2-} + 3H_2O$	+0.276
$Se_2Cl_2 + 2e^- \rightarrow 2Se(s) + 2Cl^-$	+1.1
$Se(s) + 2H^+ + 2e^- \rightarrow H_2Se$	−0.40
$Se(s) + H^+ + 2e^- \rightarrow HSe^-$	−0.510
$Se(s) + 2e^- \rightarrow Se^{2-}$	−0.92
$Se(s) + 2H^+ + 2e^- \rightarrow H_2Se(g)$	−0.369

Table 2.3 Tellurium reactions [$TeO_2aq(s)$ refers to hydrated TeO_2 crystals]

Half-reaction	Standard or formal potential (V vs. SHE at 25 °C)
$H_2TeO_4 + 6H^+ + 2e^- \rightarrow Te^{4+} + 4H_2O$	+0.920
$H_2TeO_4 + 3H^+ + 2e^- \rightarrow HTeO_2^+ + 2H_2O$	+0.953
$H_2TeO_4 + H^+ + 2e^- \rightarrow HTeO_3^- + H_2O$	+0.631
$HTeO_4^- + 2H^+ + 2e^- \rightarrow HTeO_3^- + H_2O$	+0.813
$HTeO_4^- + H^+ + 2e^- \rightarrow TeO_3^{2-} + H_2O$	+0.584
$TeO_4^{2-} + 2H^+ + 2e^- \rightarrow TeO_3^{2-} + H_2O$	+0.892
$H_2TeO_4 + 2H^+ + 2e^- \rightarrow TeO_2(s) + 2H_2O$	+1.020
$H_2TeO_4 + 2H^+ + 2e^- \rightarrow TeO_2aq(s) + 2H_2O$	+0.854
$HTeO_4^- + 3H^+ + 2e^- \rightarrow TeO_2(s) + 2H_2O$	+1.202
$HTeO_4^- + 3H^+ + 2e^- \rightarrow TeO_2aq(s) + 2H_2O$	+1.036
$TeO_4^{2-} + 4H^+ + 2e^- \rightarrow TeO_2(s) + 2H_2O$	+1.509
$TeO_4^{2-} + 4H^+ + 2e^- \rightarrow TeO_2aq(s) + 2H_2O$	+1.343
$TeO_3(s) + 2H^+ + 2e^- \rightarrow TeO_2(s) + H_2O$	+1.020
$TeO_3(s) + 2H^+ + 2e^- \rightarrow TeO_2aq(s) + H_2O$	+0.850
$Te^{4+} + 4e^- \rightarrow Te(s)$	+0.584 (2–3 M HCl), +0.568, +0.556
$HTeO_2^+ + 3H^+ + 4e^- \rightarrow Te(s) + 2H_2O$	+0.551
$H_2TeO_3 + 4H^+ + 4e^- \rightarrow Te(s) + 3H_2O$	+0.589
$HTeO_3^- + 5H^+ + 4e^- \rightarrow Te(s) + 3H_2O$	+0.713
$TeO_3^{2-} + 6H^+ + 4e^- \rightarrow Te(s) + 3H_2O$	+0.827
$TeO_2(s) + 4H^+ + 4e^- \rightarrow Te(s) + 2H_2O$	+0.521
$TeO_2aq(s) + 4H^+ + 4e^- \rightarrow Te(s) + 2H_2O$	+0.604

Table 2.3 (continued)

Half-reaction	Standard or formal potential (V vs. SHE at 25 °C)
$Te(OH)_6^{2-} + 4e^- \rightarrow Te(s) + 6OH^-$	−0.412
$TeCl_6^{2-} + 4e^- \rightarrow Te(s) + 6Cl^-$	+0.55, +0.630 (2–3 M HCl)
$2Te^{4+} + 10e^- \rightarrow Te_2^{2-}$	+0.286
$2\,HTeO_2^+ + 6H^+ + 10e^- \rightarrow Te_2^{2-} + 4H_2O$	+0.273
$2\,HTeO_3^- + 10H^+ + 10e^- \rightarrow Te_2^{2-} + 6H_2O$	+0.402
$2\,TeO_3^{2-} + 12H^+ + 10e^- \rightarrow Te_2^{2-} + 6H_2O$	+0.493
$Te^{4+} + 2H^+ + 6e^- \rightarrow H_2Te$	+0.132
$HTeO_2^+ + 5H^+ + 6e^- \rightarrow H_2Te + 2H_2O$	+0.121
$Te^{2+} + 2e^- \rightarrow Te(s)$	+0.40
$Te_2S + 2e^- \rightarrow 2Te(s) + S^{2-}$	−0.90
$2Te(s) + 2e^- \rightarrow Te_2^{2-}$	−0.840, −0.790, −0.74
$2Te(s) + 2H^+ + 2e^- \rightarrow H_2Te_2$	−0.365 (30 °C)
$3Te_2 + 8e^- \rightarrow 2Te_2^{2-} + 2Te^{2-}$	−0.92
$Te(s) + 2H^+ + 2e^- \rightarrow H_2Te$	−0.739, −0.50 (30 °C)
$Te(s) + 2H^+ + 2e^- \rightarrow H_2Te(g)$	−0.717
$Te(s) + 2e^- \rightarrow Te^{2-}$	−0.913, –1.14
$Te_2^{2-} + 4H^+ + 2e^- \rightarrow 2H_2Te$	−0.638
$Te_2^{2-} + 2H^+ + 2e^- \rightarrow 2HTe^-$	−0.795
$Te_2^{2-} + 4H^+ + 2e^- \rightarrow 2H_2Te(g)$	−0.595
$Te_2^{2-} + 2e^- \rightarrow 2Te^{2-}$	−1.445

2.1.2 Pourbaix Diagram for Sulfur–Water

Solid substances considered: S (sulfur, light yellow, orthorhombic).

Dissolved (*in aquo*) sulfur substances considered:

H_2S (hydrogen sulfide, colorless), HS^- (hydrogen sulfide ion, colorless), S^{2-} (sulfide ion, colorless), S_2^{2-} (disulfide ion, orange), S_3^{2-} (trisulfide ion, orange), S_4^{2-} (tetrasulfide ion, orange), S_5^{2-} (pentasulfide ion, orange), $H_2S_2O_3$ (thiosulfuric acid, colorless), $HS_2O_3^-$ (acid thiosulfate ion, colorless), $S_2O_3^{2-}$ (thiosulfate ion, colorless), $S_5O_6^{2-}$ (pentathionate ion, colorless), $S_4O_6^{2-}$ (tetrathionate ion, colorless), $HS_2O_4^-$ (acid dithionite ion, colorless), $S_2O_4^{2-}$ (dithionite ion, colorless), $S_3O_6^{2-}$ (trithionate ion, colorless), H_2SO_3 (sulfurous acid, colorless), HSO_3^- (bisulfite ion, colorless), SO_3^{2-} (sulfite ion, colorless), $S_2O_6^{2-}$ (dithionate ion, colorless), H_2SO_4 (sulfuric acid, colorless), HSO_4^- (bisulfate ion, colorless), SO_4^{2-} (sulfate ion, colorless), $S_2O_8^{2-}$ (dipersulfate ion, colorless).

In Fig. 2.2, the potential–pH diagram is represented for the stable equilibria of the system sulfur–water at 25 °C, i.e., equilibria comprising the forms H_2S,

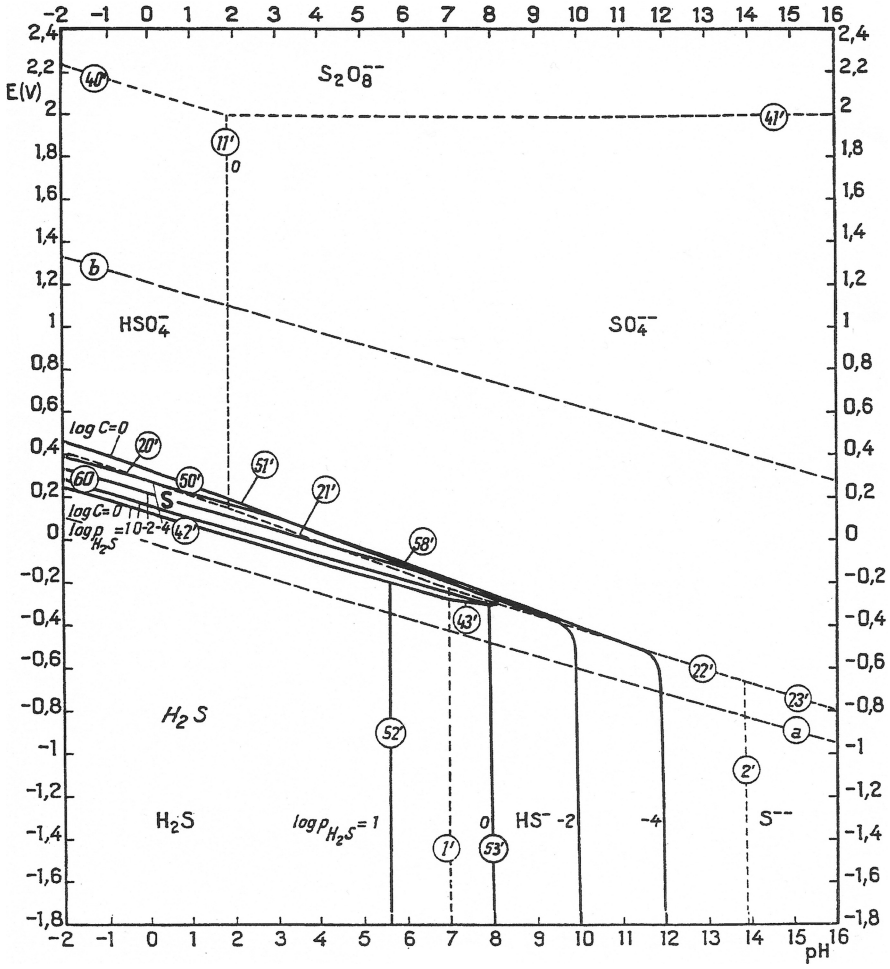

Fig. 2.2 Potential–pH diagram for the stable equilibria of the system sulfur–water at 25 °C (gaseous hydrogen sulfide is designated in *italic letters*) (Reproduced from [3], Copyright NACE International 2010)

HS^-, S^{2-}, S, HSO_4^-, SO_4^{2-}, and $S_2O_8^{2-}$, which contain sulfur only in the oxidation states –2 and +6 (aside from the solid element); other species, such as thiosulfates, dithionites, sulfites, and polythionates are in "false" equilibrium in aqueous solution. Note also that the persulfates ($S_2O_8^{2-}$) are unstable in water, so that if the equilibria were attained, only the remaining six forms would be present in solution. The limits of the domains of relative predominance of the dissolved substances included in the Pourbaix diagram (plus solid sulfur) regard the following homogeneous and heterogeneous (solid/liquid, gas/liquid) equilibria, involving redox and non-redox processes:

Limits of the domains of relative predominance of dissolved substances	*Redox equilibria*
(**1′**) H_2S/HS^-	(**41′**) $S_2O_8^{2-} + 2e^- \rightarrow 2SO_4^{2-}$
(**2′**) HS^-/S^{2-}	(**40′**) $S_2O_8^{2-} + 2H^+ + 2e^- \rightarrow 2HSO_4^-$
(**52′**) $H_2S(g)/H_2S(aq)$	(**50′**) $HSO_4^- + 7H^+ + 6e^- \rightarrow S(s) + 4H_2O$
(**53′**) $H_2S(g)/HS^-$	(**51′**) $SO_4^{2-} + 8H^+ + 6e^- \rightarrow S(s) + 4H_2O$
(**11′**) HSO_4^-/SO_4^{2-}	(**20′**) $HSO_4^- + 9H^+ + 8e^- \rightarrow H_2S(aq) + 4H_2O$
	(**21′**) $SO_4^{2-} + 10H^+ + 8e^- \rightarrow H_2S(aq) + 4H_2O$
	(**22′**) $SO_4^{2-} + 9H^+ + 8e^- \rightarrow HS^- + 4H_2O$
	(**23′**) $SO_4^{2-} + 8H^+ + 8e^- \rightarrow S^{2-} + 4H_2O$
	(**58′**) $SO_4^{2-} + 10H^+ + 8e^- \rightarrow H_2S(g) + 4H_2O$
	(**42′**) $S(s) + 2H^+ + 2e^- \rightarrow H_2S(aq)$
	(**60**) $S(s) + 2H^+ + 2e^- \rightarrow H_2S(g)$
	(**43′**) $S(s) + H^+ + 2e^- \rightarrow HS^-$

2.1.3 Pourbaix Diagram for Selenium–Water

Solid substances considered: Se (selenium, gray, trigonal).

Dissolved (*in aquo*) selenium substances considered:

H_2Se (hydrogen selenide, colorless), HSe^- (acid telluride ion, colorless), Se^{2-} (selenide ion, colorless), H_2SeO_3 (selenous acid, colorless), $HSeO_3^-$ (acid selenite ion, colorless), SeO_3^{2-} (selenite ion, colorless), H_2SeO_4 (selenic acid, colorless), $HSeO_4^-$ (acid selenate ion, colorless), SeO_4^{2-} (selenate ion, colorless).

Limits of the domains of relative predominance of dissolved substances	*Redox equilibria*
1′ HSe^-/H_2Se	**12′** $HSeO_4^- + 3H^+ + 2e^- \rightarrow H_2SeO_3 + H_2O$
2′ Se^{2-}/HSe^-	**13′** $SeO_4^{2-} + 4H^+ + 2e^- \rightarrow H_2SeO_3 + H_2O$
3′ $HSeO_3^-/H_2SeO_3$	**14′** $SeO_4^{2-} + 3H^+ + 2e^- \rightarrow HSeO_3^- + H_2O$
4′ $SeO_3^{2-}/HSeO_3^-$	**15′** $SeO_4^{2-} + 2H^+ + 2e^- \rightarrow SeO_3^{2-} + H_2O$
6′ $SeO_4^{2-}/HSeO_4^-$	**19** $H_2SeO_3 + 4H^+ + 4e^- \rightarrow Se(s) + 3H_2O$
24 $HSe^-/H_2Se(g)$	**20** $HSeO_3^- + 5H^+ + 4e^- \rightarrow Se(s) + 3H_2O$
	21 $SeO_3^{2-} + 6H^+ + 4e^- \rightarrow Se(s) + 3H_2O$
	7′ $H_2SeO_3 + 6H^+ + 6e^- \rightarrow H_2Se + 3H_2O$
	8′ $HSeO_3^- + 7H^+ + 6e^- \rightarrow H_2Se + 3H_2O$
	9′ $HSeO_3^- + 6H^+ + 6e^- \rightarrow HSe^- + 3H_2O$
	10′ $SeO_3^{2-} + 7H^+ + 6e^- \rightarrow HSe^- + 3H_2O$
	11′ $SeO_3^{2-} + 6H^+ + 6e^- \rightarrow Se^{2-} + 3H_2O$
	16 $Se(s) + 2H^+ + 2e^- \rightarrow H_2Se$
	17 $Se(s) + H^+ + 2e^- \rightarrow HSe^-$
	18 $Se(s) + 2e^- \rightarrow Se^{2-}$
	22 $Se(s) + 2H^+ + 2e^- \rightarrow H_2Se(g)$

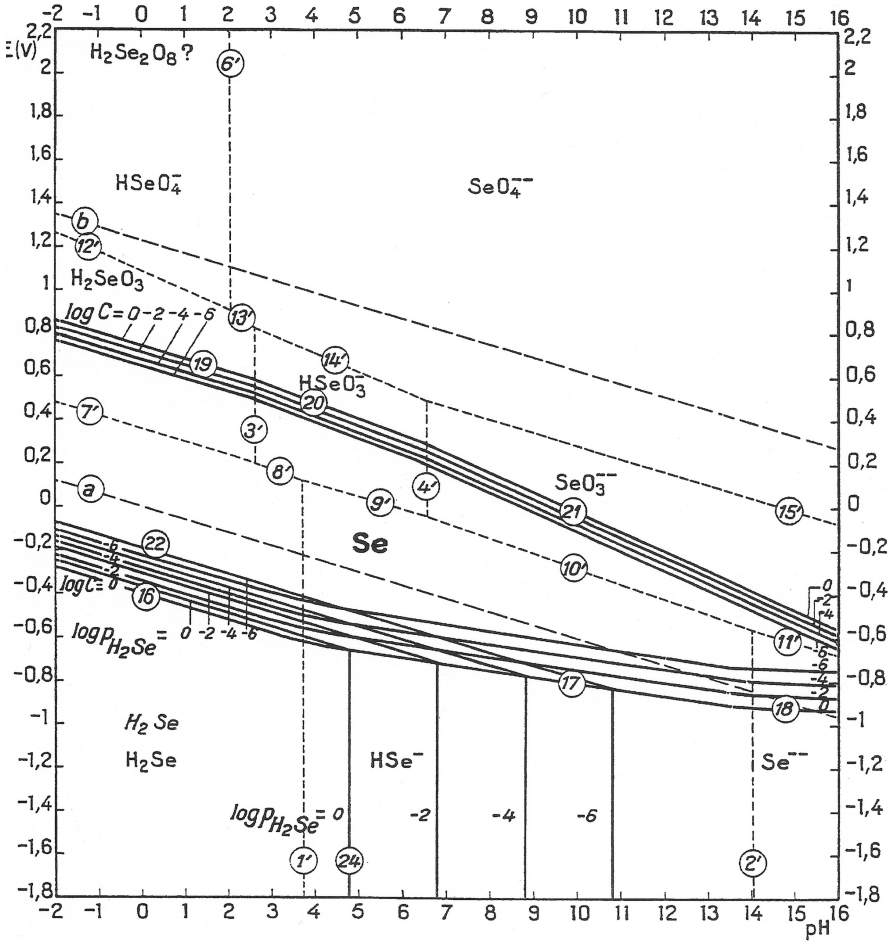

Fig. 2.3 Potential–pH equilibrium diagram for the system selenium–water, at 25 °C (gaseous hydrogen selenide is designated in *italic letters*) (Reproduced from [3], Copyright NACE International 2010)

The potential–pH diagram for the system selenium–water at 25 °C is given in Fig. 2.3. This diagram was constructed by using the homogeneous and heterogeneous (solid/liquid, gas/liquid) equilibria listed in the previous page, in which all of the above-referred dissolved substances of selenium (as well as solid Se) participate.

2.1.4 Pourbaix Diagram for Tellurium–Water

Solid substances considered:

Te (tellurium, brown black, amorphous), TeO_2 (tellurous anhydride, white), TeO_2 hydr. (tellurous acid, H_2TeO_3 or $TeO_2 \cdot H_2O$, white, amorphous), TeO_3 hydr. (orthotelluric acid, H_6TeO_6 or $TeO_3 \cdot 3H_2O$, colorless, cubic or monoclinic).

Dissolved (*in aquo*) tellurium substances considered:

H_2Te (hydrogen telluride, colorless), HTe^- (hydrogen telluride ion, colorless), Te^{2-} (telluride ion, colorless), Te_2^{2-} (ditelluride ion, red), Te^{4+} (tellurous ion), $HTeO_2^+$ (telluryl ion), $HTeO_3^-$ (acid tellurite ion, colorless), TeO_3^{2-} (tellurite ion, colorless), H_2TeO_4 (telluric acid, colorless), $HTeO_4^-$ (acid tellurate ion, colorless), TeO_4^{2-} (tellurate ion, colorless).

The potential–pH diagram for the system tellurium–water at 25 °C is given in Fig. 2.4. It was constructed by using the following homogeneous and heterogeneous (solid/liquid, gas/liquid) equilibria, involving redox and non-redox processes, in which all of the above-referred dissolved substances of tellurium, as well as the solid ones, participate:

Limits of the domains of relative predominance of dissolved substances	*Redox equilibria*
1′ H_2Te/HTe^- **2′** HTe^-/Te^{2-} **3′** $Te^{4+}/HTeO_2^+$ **4′** $HTeO_2^+/HTeO_3^-$ **5′** $HTeO_3^-/TeO_3^{2-}$ **6′** $H_2TeO_4/HTeO_4^-$ **7′** $HTeO_4^-/TeO_4^{2-}$	**17′** $H_2TeO_4 + 6H^+ + 2e^- \rightarrow Te^{4+} + 4H_2O$ **18′** $H_2TeO_4 + 3H^+ + 2e^- \rightarrow HTeO_2^+ + 2H_2O$ **19′** $H_2TeO_4 + H^+ + 2e^- \rightarrow HTeO_3^- + H_2O$ **20′** $HTeO_4^- + 2H^+ + 2e^- \rightarrow HTeO_3^- + H_2O$ **21′** $HTeO_4^- + H^+ + 2e^- \rightarrow TeO_3^{2-} + H_2O$ **22′** $TeO_4^{2-} + 2H^+ + 2e^- \rightarrow TeO_3^{2-} + H_2O$ **38′** $H_2TeO_4 + 2H^+ + 2e^- \rightarrow TeO_2(s) + 2H_2O$ **39′** $HTeO_4^- + 3H^+ + 2e^- \rightarrow TeO_2(s) + 2H_2O$
Two dissolved substances in the presence of Te (solution saturated with elementary Te) **8″** H_2Te/Te_2^{2-} **14″** $HTeO_2^+/Te_2^{2-}$ **15″** $HTeO_3^-/Te_2^{2-}$ **16″** TeO_3^{2-}/Te_2^{2-}	**24** $TeO_3(s) + 2H^+ + 2e^- \rightarrow TeO_2(s) + H_2$ $TeO_3(s) + 2H^+ + 2e^- \rightarrow TeO_2aq(s) + H_2O$ **34′** $Te^{4+} + 4e^- \rightarrow Te(s)$ **35′** $HTeO_2^+ + 3H^+ + 4e^- \rightarrow Te(s) + 2H_2O$ **36′** $HTeO_3^- + 5H^+ + 4e^- \rightarrow Te(s) + 3H_2O$ **37′** $TeO_3^{2-} + 6H^+ + 4e^- \rightarrow Te(s) + 3H_2O$ **23** $TeO_2(s) + 4H^+ + 4e^- \rightarrow Te(s) + 2H_2O$
One solid substance and one dissolved substance **25′** Te^{4+}/TeO_2 **26′** $HTeO_2^+/TeO_2$ **27′** $TeO_2/HTeO_3^-$ **28′** TeO_2/TeO_3^{2-}	**11′** $Te^{4+} + 2H^+ + 6e^- \rightarrow H_2Te$ **12′** $HTeO_2^+ + 5H^+ + 6e^- \rightarrow H_2Te + 2H_2O$ **33′** $2Te(s) + 2e^- \rightarrow Te_2^{2-}$ **32′** $Te(s) + 2H^+ + 2e^- \rightarrow H_2Te$ **45′** $Te(s) + 2H^+ + 2e^- \rightarrow H_2Te(g)$
One gaseous substance and one dissolved substance **42′** $H_2Te(g)/HTe^-$	**8′** $Te_2^{2-} + 4H^+ + 2e^- \rightarrow 2H_2Te$ **9′** $Te_2^{2-} + 2H^+ + 2e^- \rightarrow 2HTe^-$ **44′** $Te_2^{2-} + 4H^+ + 2e^- \rightarrow 2H_2Te(g)$ **10′** $Te_2^{2-} + 2e^- \rightarrow 2Te^{2-}$

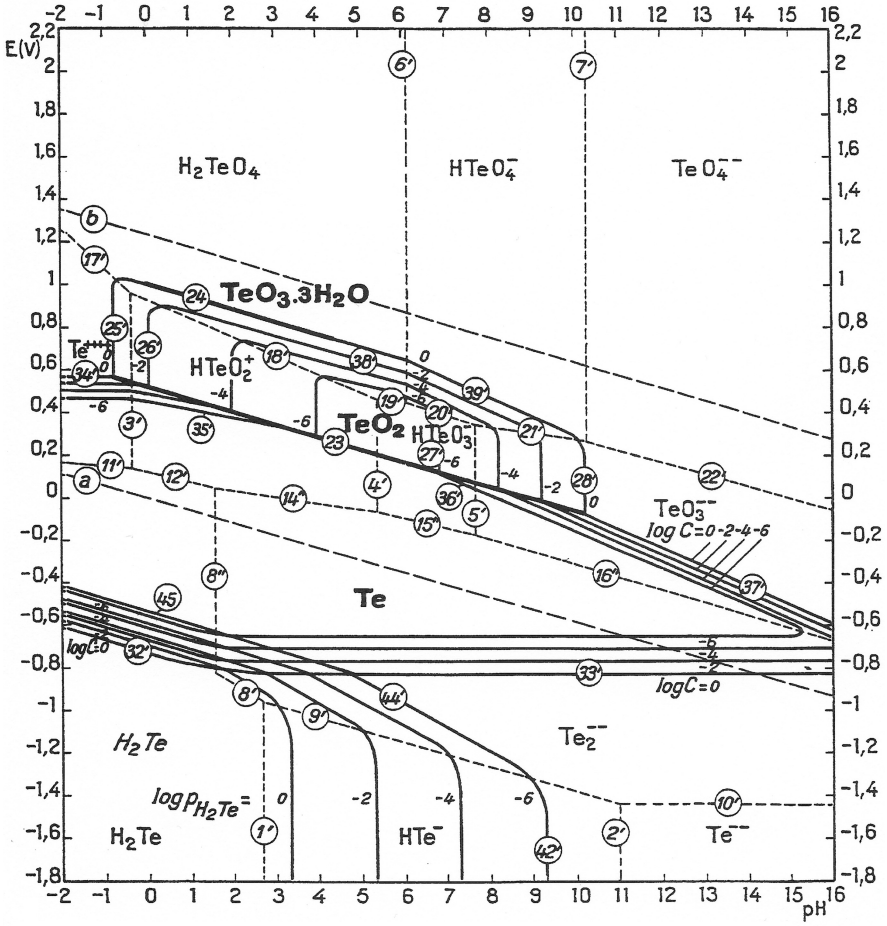

Fig. 2.4 Potential–pH equilibrium diagram for the system tellurium–water, at 25 °C. (The form of TeO_2 considered in this diagram is the anhydrous one, which is more stable than the hydrated form $TeO_2 \cdot H_2O$. Gaseous hydrogen telluride is designated in *italic letters*) (Reproduced from [3], Copyright NACE International 2010)

2.2 General Discussion

2.2.1 Sulfur

In the Pourbaix diagram, solid sulfur appears to be stable in a very narrow triangular domain, which lies completely within the stability domain of water. Sulfur is therefore stable in the presence of water and in acid solutions free from oxidizing agents. It is unstable, however, in alkaline solutions, in which it tends to disproportionate to give HS^-, S^{2-} (and polysulfides), SO_4^{2-}, and other oxidation products. In

practice, these reactions are slow and take place only in hot, very alkaline media. The sulfides of the alkali metals and the alkaline earth metals are soluble in water, whereas the other sulfides are insoluble but dissolve in varying degrees in acid solutions.

The various oxidation states of sulfur have been determined by polarography. The electrochemical oxidation of sulfide ions in aqueous solution may lead to the production of elementary sulfur, polysulfides, sulfate, dithionate, and thiosulfate, depending on the experimental conditions. Disulfides, sulfoxides, and sulfones are typical polarographically active organic compounds. It is also found that thiols (mercaptans), thioureas, and thiobarbiturates facilitate oxidation of Hg resulting thus in anodic waves.

The electroreduction behavior of elemental sulfur with formation of polysulfide anions in classical organic solvents (DMF, DMA, DMSO, CH_3CN, etc.) as well as in liquid ammonia is well documented [5]. Significant progress has been achieved in the interpretation of this process in dimethylformamide (DMF) [6]. On the other hand, electrooxidation of the element to form polysulfur cations is only known in molten salts and in fluorosulfuric acid [7]. The electrochemical disproportionation of sulfur has been studied in strongly basic media, e.g., in $NaOH+H_2O$ melts [8, 9]. A large number of investigations regard the electrochemical properties of the sulfur–sulfide system in molten mixtures of sulfur and polysulfide [10] or molten chlorides [11, 12] in connection with the production of alkali sulfur batteries (Chap. 6).

The very low solubility of elemental sulfur in water does not allow the study of its electrochemical reduction in aqueous media. Thus, the electrochemical behavior of sulfide (HS^-, S^{2-}) and polysulfide ions in water is much less documented than for non-aqueous solvents, while the relevant investigations bare often speculative conclusions since the experimental results do not display strong evidence for chemical species involved in the proposed mechanisms. Anyhow, a number of investigations have been carried out on the electrochemical properties of the aqueous sulfur–sulfide system on different substrate electrodes regarding the involved redox behavior, the formation or adsorption of sulfur and sulfur species on the electrodes, and speciation of sulfur species in solution or on the electrode surface. Differences in the method of formation of sulfur layers, stimulated by diverse interests, have led to apparently conflicting observations regarding, for example, the formation or not of polysulfide species as intermediates in the oxidation of sulfide ions to sulfur [13–16]. Analogous dispute is found for the electroreduction of sulfur to sulfide ions [17, 18], since the understanding of these processes requires the unambiguous identification of the reduced forms of sulfur, i.e., polysulfides.

The surface chemistry of sulfur on metals has been intensively studied as being extremely important in several technologies, including metallurgy, metal corrosion, and heterogeneous catalysis. For example, alkali sulfides have been widely used for a long time in the flotation of base metal oxide and sulfide minerals [19, 20]; or well known are the corrosive effects of sulfide ions on iron based alloys during the processing of crude oil and natural gas. The adsorption of sulfur on metal surfaces may have a remarkable effect on the surface reactivity, notably on the electrochemical

properties. Well documented is the effect of sulfur adsorbent layers on the anodic dissolution rate of metals such as copper, silver, gold, nickel or on the conditions for silver electrodeposition, the overvoltage for hydrogen evolution on nickel and iron, etc. (see previous references). The blocking effect of sulfur on hydroxyl adsorption sites of the electrode with subsequent inhibition of the electrochemical oxidation reaction (passivation) is well known, as also is the inhibitory effect of sulfur layers on the electrocatalytic activity of noble metals (especially when the reactants are strongly adsorbed on the electrode). Interestingly, it has been observed that adsorbed sulfur significantly enhances the electrocatalytic activity of some metals causing an increase in the reaction rates. The electroreduction of ferric ions on Pt electrodes in acid media has been used as a model reaction for investigation of the effect of chemisorbed sulfur on the charge transfer across the metal–solution interface. This effect has been interpreted on the basis of the Marcus theory of electron transfer [21, 22].

In the context of environmental chemistry, various polarographic techniques have been successfully used to measure elemental sulfur and sulfide (H_2S and HS^-) concentrations in a variety of media, down to nanomolar concentrations.

Redox reactions of sulfur involving reduction–oxidation of sulfate, sulfide, and sulfur species/clusters are of extreme biological, geochemical, and environmental importance. The progress in the electrochemistry of sulfido-clusters is connected with better understanding of the processes that occur in living systems with involvement of transition metals, since at least seven of those (V, Mo, W, Fe, Ni, Cu, and Zn) are bonded quite often to sulfur (and/or selenium) atoms and are vital for various biological functions. For example, the association of sulfur and iron into simple to more complex molecular assemblies allows a great flexibility of electron transfer relays and catalysis in metalloproteins, which play a major role in terminal respiration, photosynthesis, and dinitrogen reduction. Iron–sulfur cluster synthesis in the laboratory and the subsequent study of their electrochemical properties has been stimulated by the occurrence and characterization of such centers in many redox enzymes and provides, in turn, valuable insight into natural reaction mechanisms [23].

2.2.2 Selenium

Selenium is stable in water and in aqueous solutions over the entire pH interval in the absence of any oxidizing or reducing agent. Selenium can be electrochemically reduced to hydrogen selenide or to selenides that are unstable in water and aqueous solutions. It can be oxidized to selenous acid or selenites and further (electrolytically) to perselenic acid ($H_2Se_2O_8$). Selenic and selenous acids and their salts are stable in water. The selenides, selenites, and selenates of metals other than the alkali metals are generally insoluble.

The polarographic behavior of selenium in aqueous solutions has been studied in great detail, being in fact far simpler than that of sulfur because the selenium compounds exhibit electrochemical activity essentially in only two different

valent states, i.e., Se(–II) and Se(+IV) [24, 25]. In polarography, the number and shape of the recorded waves as well as the half-wave potential values are influenced considerably by the composition and pH of the solution, mainly through variations in the distribution of the possible solution species (H_2Se, HSe^-, Se^{2-}, SeO_3^{2-}, $HSeO_3^-$, H_2SeO_3). Quadrivalent selenium exhibits polarographic waves in a number of electrolytes including hydrochloric, sulfuric, nitric, and perchloric acids, potassium nitrate, ammonium acetate, ammonia–ammonium chloride, and orthophosphate buffer solutions [26].

As with sulfur, deposition of Se monolayers tends to passivate electrode surfaces. Selenide compound formation involving the electrode material was evident already from the early studies. Thus, changes in the polarographic waves of Se(IV) upon standing were attributed to the formation of "HgSe" compound [27], while other electrode materials, such as Ag, Cd, Cu, and In, are all known to react chemically with either Se(0) or Se(–II) species. Some electrodes (e.g., Au) promote the UPD of Se(0) via strong metal–Se interactions: Andrews and Johnson [28] reported two waves for the reduction of Se(IV) at an Au electrode in 0.1 M $HClO_4$; the one at the more positive potential was assigned to a UPD process. The authors argued that the electrodeposition of Se(IV) produces Se in three distinct states of activity, one by one corresponding to the three anodic stripping peaks observed for large quantities of deposited Se. The authors claimed that, in effect, approximately a monolayer is initially deposited which is stabilized by 1D interaction with the Au electrode surface. The formation of a bulk deposit produces a large activity gradient which is the driving force for irreversible diffusional transport of Se into the Au electrode forming Au–Se alloy of unknown stoichiometry. Surface-adsorbed selenium and bulk selenium correspond, respectively, to the other two activity states detected by stripping voltammetry.

The mechanism of Se(IV) reduction has been debated a lot in the last four decades. The early polarographic data, as also most recent voltammetric studies, were interpreted in terms of a two-step Se(+IV) → Se(0) → Se(–II) scheme, where the reduction of Se(0) takes place at the more negative potentials. However, electroreduction of Se(IV), being generally more sluggish than of Te(IV), tends to favor a direct six-electron route at relatively positive potentials. In fact, as first recognized by Skyllas-Kazacos and Miller [29], and emphasized by Wei et al. [30], the $6e^-$ process generating Se(–II) ions, although not recognized in the majority of the earlier studies at least in neutral and acidic media, is considered very likely to occur in competition to the $4e^-$ reduction pathway. Certainly, for a given bath composition, voltammetric or other experiments may reveal which reaction will predominate at any potential.

The observed complexity of the Se(IV) electrochemistry due to adsorption layers, formation of surface compounds, coupled chemical reactions, lack of electroactivity of reduction products, and other interrelated factors has been discussed extensively. Zuman and Somer [31] have provided a thorough literature-based review with almost 170 references on the complex polarographic and voltammetric behavior of Se(+IV) (selenous acid), including the acid–base properties, salt and complex formation, chemical reduction and reaction with organic and inorganic

sulfur compounds, polarographic and stripping analysis in the presence of heavy metal ions, as well as the principles and applications of stripping analyses for determination of ultratraces of Se(IV). Important information was given also on the electroanalytical behavior of Se(IV) on gold, silver, platinum, carbon, copper, titanium, and tin oxide electrodes.

Selenium films have been prepared by electrodeposition via both the cathodic and anodic routes. An informative report embodying findings of early practical work has been given by von Hippel and Bloom [32] who used aqueous selenous/selenic acid mixtures as plating baths. These authors pointed out that the main obstacle in electroplating selenium lies in the polymorphism of the element, and that unless special conditions are chosen the material deposits as a non-conductor and interrupts the current flow. They also reported that the electrodeposition of amorphous selenium practically ceases in the dark but could be continued under strong illumination. Graham et al. [33] described the deposition of thick amorphous Se deposits from SeO_2 baths containing a surfactant agent. A serious drawback was the short life of the bath before defective deposits were obtained. The nature of the cathode material was seen to exert a profound influence on the appearance and structure of the deposits. Bright-nickel plating was the best of the substrates examined, which included Pb, Ag, Au, Rh, Cu, dull Ni, bright Cr, black Cr electrodeposits, and Pt sheets. Cattarin et al. [34] studied the Se electrodeposition onto Ti electrodes from acidic selenite baths, as a function of SeO_2 concentration, presence of surfactant, electrode illumination, and temperature. Cyclic voltammetry showed a reduction peak followed by a "passive" and then a "transpassive" domain at more negative potentials. Growth of the Se film at potentials within the "reduction" domain stopped at a limiting thickness. The film could be grown further in the "transpassive" potential domain.

Trigonal, "metallic" selenium has been investigated as photoelectrode for solar energy conversion, due to its semiconducting properties. The photoelectrochemistry of the element has been studied in some detail by Gissler [35]. A photodecomposition reaction of Se into hydrogen selenide was observed in acidic solutions. Only redox couples with a relatively anodic standard potential could prevent dissolution of Se crystal.

2.2.3 Tellurium

Tellurium is stable in the presence of water and aqueous solutions free from oxidizing agents, except in very alkaline solutions, in which it is possible to dissolve with the simultaneous formation of tellurite, TeO_3^{2-}, and ditelluride, Te_2^{2-}, ions. In oxygenated water, tellurium becomes covered with the dioxide TeO_2, which is non-protective if the tellurium is freshly precipitated, but in the compact state it constitutes a protective film. Tellurium can be cathodically reduced in acid solution to give dissolved and gaseous hydrogen telluride or in alkaline solution to give Te_2^{2-} and possibly Te^{2-} ions. It can be anodically oxidized to tellurous anhydride TeO_2 (sparingly soluble at pH around 4–7) or to the telluric oxide (orthotelluric

acid; very soluble), telluric acid, and tellurates. Tellurous ions can be obtained in very acidic solutions. The tellurides, tellurites, and tellurates of metals other than the alkali metals are generally insoluble.

On account of its electrochemically active valent states, tellurium exhibits a very interesting polarographic behavior. Lingane and Niedrach [25], in their fundamental study on dc polarography and controlled potential coulometry in tellurous acid solutions, have shown that, except for strongly alkaline medium, the reduction of Te(+IV) occurs via a four-electron process to tellurium, whereas in sodium hydroxide solutions, Te^{2-} results via a $6e^-$ direct reduction. The presence of a sharp and intense maximum on the wave plateau of acidic or neutral pH media was attributed to the Te/Te(–II) couple, but some difficulties in a correct interpretation arose. Regarding telluride solutions, a practically reversible oxidation of Te^{2-} to the elemental state was noted in the full range of pH [24]. Shinagawa et al. [36, 37] discussed the Te(IV) reduction mechanism in weakly basic solutions, emphasizing that the two-step reduction to Te(0) and further to Te(–II) at the mercury drop electrode is complicated by the adsorption of elemental tellurium at the mercury surface (see also [38–40]). The authors pointed out the influence of UV irradiation on the first reduction step. Panson [41] investigated the polarographic behavior of the ditelluride ion prepared by cathodic dissolution of Te in alkaline solution and noted its disproportionation to Te and Te^{2-}.

Lingane and Niedrach have claimed that the +VI states of tellurium (or selenium) are not reduced at the dropping electrode under any of the conditions of their investigation; however, Norton et al. [42] showed that under a variety of conditions, samples of telluric acid prepared by several different procedures do exhibit well-defined (though irreversible) waves, suitable for the analytical determination of the element. The reduction of Te(+VI) at the dropping electrode was found coulometrically to proceed to the –II state (whereas selenate, Se(+VI), was not reduced at the dropping electrode in any of the media reported).

Numerous voltammetric investigations can be found on the electrochemistry of tellurium in aqueous electrolytes and various metals, glassy carbon, or Te electrodes, discussing the mechanism of Te(IV) reduction to Te(0) or the cathodic and anodic stripping of the element (e.g., [43–46]). It is generally accepted that in acid aqueous media the Te(+IV) is present in the form of the telluryl ion $HTeO_2^+$. Experimental data for the solubility and diffusivity of $HTeO_2^+$ have been reported by use of the electrohydrodynamical (EHD) impedance method [47]. In most works, it is assumed that at low pH, the telluryl ion may be electrochemically reduced to give elementary tellurium via a process that takes place in one step with the transfer of four electrons [48]. Further reduction of the formed Te at more negative potentials leads to the H_2Te species and simultaneous hydrogen evolution. In addition, a conproportionation reaction between Te(IV) and Te(–II) appears to give Te(0) deposited on the electrode. Other authors have proposed that the telluryl ion is electrochemically reduced by a direct six-electron transfer to form the H_2Te species, which then reacts chemically with the telluryl ion to give elementary tellurium on the cathode [49, 50]. In any case, using a combination of voltammetry and electrochemical quartz crystal microgravimetry (EQCM), Mori et al. [51] argued that the six-electron reduction

pathway is important and must be considered in the overall mechanistic scheme of electroreduction for both Te(IV) and Se(IV).

The possibility that adsorption reactions play an important role in the reduction of telluryl ions has been discussed in several works (Chap. 3; CdTe). By using various electrochemical techniques in stationary and non-stationary diffusion regimes, such as voltammetry, chronopotentiometry, and pulsed current electrolysis, Montiel-Santillán et al. [52] have shown that the electrochemical reduction of $HTeO_2^+$ in acid sulfate medium (pH 2) on solid tellurium electrodes, generated in situ at 25 °C, must be considered as a four-electron process preceded by a slow adsorption step of the telluryl ions; the reduction mechanism was observed to depend on the applied potential, so that at high overpotentials the adsorption step was not significant for the overall process.

Data on the electrochemistry of the telluride ion in alkaline media are relatively limited. Mishra et al. [53] studied the oxidation of Te^{2-} to Te^0 at solid electrodes, focusing on the intermediate step(s) of this process, and in particular, the possibility of detecting ditelluride Te_2^{2-} via rotating ring disk electrode (RRDE) methodology. Oxidation beyond the elemental state to TeO_3^{2-} and TeO_4^{2-} was also studied using cyclic and hydrodynamic voltammetry.

Various classes of organotellurium compounds in aprotic solvents have been studied as to their electrochemistry, whereas more limited are the reports on the electrochemistry of tellurium and its inorganic compounds in non-aqueous solvents [54, 55].

References

1. Zhdanov I (1975) Sulfur. In Bard AJ (ed) Encyclopedia of electrochemistry of the elements, Marcel Dekker, New York (Vol 4, pp. 273–360); Selenium. *Ibid* (pp. 361–392); Tellurium. *Ibid* (pp. 393–443)
2. Latimer WM (1952) The oxidation states of the elements and their potentials in aqueous solutions. 2nd edn. Prentice Hall, New York
3. Pourbaix M (1974) Atlas of electrochemical equilibria in aqueous solutions. National association of corrosion engineers (2nd English Edn.) USA
4. L'Her M (2006) Redox Properties, Electrochemistry of Oxygen. In Bard AJ, Stratmann M (eds) Encyclopedia of Electrochemistry, Vol. 7a: Inorganic Chemistry, Scholz F, Pickett ChJ (eds), Wiley-VCH, Weinheim, p 117
5. Demortier A, Lelieur J-P, Levillain E (2006) Sulfur. In Bard AJ, Stratmann M (eds) Encyclopedia of Electrochemistry, Vol. 7a: Inorganic Chemistry, Scholz F, Pickett ChJ (eds), Wiley-VCH, Weinheim, p 253
6. Levillain E, Gaillard F, Leghie P, Demortier A, Lelieur JP (1997) On the understanding of the reduction of sulfur (S_8) in dimethylformamide (DMF). J Electroanal Chem 420: 167–177
7. Fehrmann R, Bjerrum NJ, Poulsen FW (1978) Lower oxidation states of sulfur. 1. Spectrophotometric study of the sulfur-chlorine system in molten sodium chloride-aluminum chloride (37:63 mol%) at 150 °C. Inorg Chem 17: 1195–1200
8. Moscardo-Levelut MN, Plichon V (1984) Sulfur chemistry in equimolar NaOH-H_2O melt. I. Electrochemical oxidation of sodium sulfide. J Electrochem Soc 131: 1538–1545
9. Claes P, Dewilde Y, Glibert J (1988) Chemical and electrochemical behaviour in molten alkali hydroxides: Part II. Electrochemistry of chalcogenide ions in the molten NaOH + KOH (49 mol%) eutectic mixture. J Electroanal Chem 250: 327–339

10. Dobson JC, McLarnon FR, Cairns EJ (1986) Voltammetry of sodium polysulfides at metal electrodes. J Electrochem Soc 133: 2069–2076
11. Warin D, Tomczuk Z, Vissers DR (1983) Electrochemical behavior of Li_2S in fused LiCl-KCl electrolytes. J Electrochem Soc 130: 64–70
12. Weaver MJ, Inman D (1975) The sulphur-sulphide electrode in molten salts–I: Chronopotentiometric behaviour in lithium chloride–potassium chloride eutectic. Electrochim Acta 20: 929–936
13. Allen PL, Hickling A (1957) Electrochemistry of sulphur. Part 1 – Overpotential in the discharge of the sulphide ion. Trans Faraday Soc 53: 1626–1635
14. Briceno A, Chander S (1990) Oxidation of hydrosulphide ions on gold – Part I: A cyclic voltammetry study. J Appl Electrochem 20: 506–511
15. Wierse DG, Lohrengel MM, Schultze JW (1978) Electrochemical properties of sulfur adsorbed on gold electrodes. J Electroanal Chem 92: 121–131
16. Van Huong CN, Parsons R, Marcus P, Montes S, Oudar J (1981) Electrochemical behaviour of silver and gold single-crystal surfaces covered with a monolayer of adsorbed sulphur. J Electroanal Chem 119: 137–148
17. Hamilton IC, Woods R (1983) An investigation of the deposition and reactions of sulphur on gold electrodes. J Appl Electrochem 13: 783–794
18. Buckley AN, Hamilton IC, Woods R (1987) An investigation of the sulphur(–II)/sulphur(0) system on gold electrodes. J Electroanal Chem 216: 213–227
19. Hamilton IC, Woods R (1981) An investigation of surface oxidation of pyrite and pyrrhotite by linear potential sweep voltammetry. J Electroanal Chem 118: 327–343
20. Buswell AM, Nicol MJ (2002) Some aspects of the electrochemistry of the flotation of pyrrhotite. J Appl Electrochem 32: 1321–1329
21. Samec Z, Weber J (1972) Reduction of ferric ion on a rotating platinum electrode of the turbulent type in the presence and absence of adsorbed sulfur. J Electroanal Chem Interfacial Electrochem 38: 115–126
22. Samec Z, Weber J (1973) The influence of chemisorbed sulfur on the kinetic parameters of the reduction of Fe^{3+} ions on a platinum electrode on the basis of the Marcus theory of electron transfer. J Electroanal Chem Interfacial Electrochem 44: 229–238
23. Barriére F (2006) Aspects of metallo-sulfur cluster's electrochemistry. In Bard AJ, Stratmann M (eds) Encyclopedia of Electrochemistry, Vol. 7b: Inorganic Chemistry, Scholz F, Pickett ChJ (eds), Wiley-VCH, Weinheim, p 591
24. Lingane JJ, Niedrach LW (1948) Polarography of selenium and tellurium. I. The –2 States. J Am Chem Soc 70: 4115–4120
25. Lingane JJ, Niedrach LW (1949) Polarography of selenium and tellurium. II. The + 4 States. J Am Chem Soc 71: 196–204
26. Christian GD, Knoblock EC, Purdy WC (1963) Polarography of selenium(IV). Anal Chem 35: 1128–1132
27. Christian GD, Knoblock EC, Purdy WC (1965) Use of highly acid supporting electrolytes in polarography. Observed changes in polarographic waves of selenium(IV) upon standing. Anal Chem 37: 425–427
28. Andrews RW, Johnson DC (1975) Voltammetric deposition and stripping of selenium(IV) at a rotating gold-disk electrode in 0.1 M perchloric acid. Anal Chem 47: 294–299
29. Skyllas-Kazacos M, Miller B (1980) Studies in selenous acid reduction and CdSe film deposition. J Electrochem Soc 127: 869–873
30. Wei C, Myung N, Rajeshwar K (1994) A combined voltammetry and electrochemical quartz crystal microgravimetry study of the reduction of aqueous Se(IV) at gold. J Electroanal Chem 375: 109–115
31. Zuman P, Somer G (2000) Polarographic and voltammetric behavior of selenous acid and its use in analysis. Talanta 51: 645–665
32. von Hippel A, Bloom MC (1950) The electroplating of metallic selenium. J Chem Phys 18: 1243–1251

33. Graham AK, Pinkerton HL, Boyd HJ (1959) Electrodeposition of amorphous selenium. J Electrochem Soc 106: 651–654
34. Cattarin S, Furlanetto F, Musiani MM (1996) Cathodic electrodeposition of Se on Ti electrodes. J Electroanal Chem 415: 123–132
35. Gissler W (1980) Photoelectrochemical investigation on trigonal selenium film electrodes. J Electrochem Soc 127: 1713–1716
36. Shinagawa M, Yano N, Kurosu T (1972) Mechanism and analytical aspects of the polarographic maximum wave of tellurium. Talanta 19: 439–450.
37. Shinagawa M, Sorarnasu N, Mori Y, Okuma T (1977) Studies on the prewave of tellurium and its photo-effect. J Electroanal Chem 75: 809–817
38. Volaire M, Vittori O, Porthault M (1974) Determination du tellure (IV) en milieu acide par polarographie à tension alternative impulsionnelle et par voltammétrie à balayage linéaire. Anal Chim Acta 71: 185–191
39. Vittori O (1980) Polarographic study of adsorbed tellurium at the hanging and dropping mercury electrodes in 1 M hydrochloric or perchloric acid solutions. Anal Chim Acta 121: 315–319
40. Sarala Y, Reddy SJ (1986) Electrochemical reduction of tellurium (IV). J Electroanal Chem 214: 179–190
41. Panson AJ (1963) Polarography of the ditelluride ion. J Phys Chem 67: 2177–2180
42. Norton E, Stoenner RW, Medalia AI (1953) Polarography of tellurium (VI). J Am Chem Soc 75: 1827–1830
43. Traore M, Moddo R, Vittori O (1988) Electrochemical behaviour of tellurium and silver telluride at rotating glassy carbon electrode. Electrochim Acta 33: 991–996
44. Ngać N, Vittori O, Quarin G (1984) Voltammetric and chronoamperometric studies of tellurium electrodeposition of glassy carbon and gold electrodes. J Electroanal Chem 167: 227–235
45. Barbier MJ, Becdelievre AM, Becdelievre J (1978) Electrochemical study of tellurium oxidoreduction in aqueous solutions. J Electroanal Chem 94: 47–57
46. Dergacheva MB, Statsyuk VN, Fogel LA (2001) Electroreduction of tellurium (IV) on solid electrodes in neutral solutions. Russ J Electrochem 37: 626–628
47. Deslouis C, Maurin G, Pebere N, Tribollet B (1988) Investigation of tellurium electrocrystallization by EHD impedance technique. J Appl Electrochem 18: 745–750
48. Yagi I, Nakabayashi S, Uosaki K (1998) In situ optical second harmonic rotational anisotropy measurements of an Au(111) electrode during electrochemical deposition of tellurium. J Phys Chem B 102: 2677–2683
49. Gregory WB, Norton ML, Stickney JL (1990) Thin-layer electrochemical studies of the underpotential deposition of cadmium and tellurium on polycrystalline Au, Pt and Cu electrodes. J Electroanal Chem 293: 85–101
50. Dennison S, Webster S (1992) An investigation into the effect of ionic species on the deposition of tellurium and the formation of cadmium telluride. J Electroanal Chem 333: 287–298
51. Mori E, Baker CK, Reynolds JR, Rajeshwar K (1988) Aqueous electrochemistry of tellurium at glassy carbon and gold: A combined voltammetry-oscillating quartz crystal microgravimetry study. J Electroanal Chem 252: 441–451
52. Montiel-Santillán T, Solorza O, Sánchez H (2002) Electrochemical research on tellurium deposition from acid sulfate medium. J Solid State Electrochem 6: 433–442
53. Mishra KK, Ham D, Rajeshwar K (1990) Anodic oxidation of telluride ions in aqueous base: A rotating ring-disk electrode study. J Electrochem Soc 137: 3438–3441
54. Liftman Y, Albeck M, Goldsmidt JME, Yarnitsky Ch (1984) The electrochemistry of tellurium in methylene chloride. Electrochim Acta 29: 1673–1678
55. Jeng EGS, Sun IW (1997) Electrochemistry of tellurium(IV) in the basic aluminum chloride-1-methyl-3-ethylimidazolium chloride room temperature molten salt. J Electrochem Soc 144: 2369–2374